EXPERIMENTAL STUDY OF CROSSFLOW INSTABILITY AND LAMINAR-TURBULENT TRANSITION ON A SWEPT WING

V.M. Galkin, O.V. Babitch, O.K. Shapovalov

Central Aerohydrodynamic Institute (TsAGI)
Zhukovsky, Moskow Region, Russia

Abstract

Rotating hot-wire anemometer measurements and china-clay visualization have been carried out, together with numerical study of boundary layer instability, to investigate, in detail, laminar-turbulent boundary layer transition on a swept wing model in subsonic wind tunnel. Swept wing model with 45° leading edge sweep was tested in incidence range $\alpha = -5^\circ \div 0^\circ$ and Reynolds number range $Re = 2 \div 4 \cdot 10^6$ million. Visualization showed china-clay patterns typical for stationary waves caused by cross flow instability; its developement in streamwise direction led to a series of turbulent wedges forming "shark-teeth"-like transition front. Simultaneous hot-wire measurements of cross flow and streamwise velocity profiles showed that each turbulent wedge was the continuation of a streamwise vortex with induced near-wall cross flow velocities directed backwards with respect to mean (span-averaged) boundary layer cross flow. Streamwise velocity profile across the boundary layer was extremely inflected near the center of this vortex. Linear cross flow stability calculations showed rather wide interval of transition N-factor values due to freestream turbulence level.

Introduction

Viscous drag reduction using NLF wings becomes popular in modern transonic aircraft projects. Using NLF concept in swept wing design requires detailed knowledge of swept wing transition peculiarities.

In accordance with available current knowledge, it is usual to consider several laminar-turbulent transition mechanisms in the boundary layer on a swept wing which become apparent either separately or in combination depending on wing geometry and flow conditions. Alongside with the most thoroughly studied longitudinal transition mechanism, that manifests itself in the developement of Tollmien-Schlichting waves, they include the developement of the cross flow instability, Taylor-Gortler instability on concave surfaces and attachment line transition /1/.

In the course of the investigations of the boundary layer transition the idea that the transition mechanism on swept wings may differ from the two-dimensional case was conceived in 1950s /2/.A destabilizing role of the inflected cross flow velocity profile in swept wing boundary layers was first shown in /3/. Results of /4/ demonstrated a common wave nature of a three- and two-dimensional instabilities of the laminar boundary layer, as well as the possibility of reducing the three-dimensional stability problem to an equation similar to the two-dimensional Orr-Sommerfeld equation in the coordinate system oriented in the wave disturbance vector direction. Subsequent calculations /5/-/8/ and experimental investigations /8/-/11/ have shown that a characteristic feature of the crossflow instability developement in a swept wing boundary layer is a predominant amplification of low-frequency waves with wave vectors directed at high angles to the local velocity at the external edge of the boundary layer, as well as of stationary waves. Calculated velocity disturbance streamlines showed that these waves take the form of a system of streamwise stationary vortices with the rotation direction alternating spanwise. Periodic spanwise variations in streamwise and cross flow velocity profiles, associated with this flow structure, result in respective variations of skin friction and in striped pattern of sublimating, oil or china-clay coatings used to visualize the transition /8/-/10/. In this case the transition line has a saw-toothed shape. The cross flow instability becomes most evident at a favorable pressure gradient that suppresses the developement of the longitudinal instability.

This report investigates some peculiarities of the boundary layer transition on a swept wing model. Anatomy of transition pattern is studied by simultaneous rotating hot-wire anemometer measurements and china-clay visualization in the conditions when cross flow instability is predominant.

Experimental equipment and measurement technique

The tests were carried out in the subsonic low-turbulence wind tunnel T-124 TsAGI with 1x1 m test section. The free-stream flow turbulence level did not exceed 0.05% at $V < 40$ m/s and increased up to 0.08% at $V = 80$ m/s. The swept wing model had a sweep angle $\chi = 45^\circ$ with a cross section (normal to the leading edge) having a supercritical airfoil with 0.5m chord and 12% thickness-to-chord ratio. The model was fixed in the plugs of the test section windows and could be installed at angles of attack within the range $\alpha = -6 \div +6^\circ$ due to plug rotation. The model was equipped with a drainage system to measure pressure distribution on the upper surface using pressure transducers outside the test section. For hot wire anemometer measurements, use was made of a traversing strut designed to remotely control the position of the hot-wire pick-up with respect to the model surface with an accuracy of 0.01mm in the vertical coordinate, 0.2mm in the streamwise and transverse coordinates (X_c, Y_c, Z_c is the model-fixed coordinate system with the Y_c axis perpendicular to the model surface, Fig.1) and to vary the angular orientation

of the hot wire in the X_c - Z_c plane within the range $\vartheta = -50^\circ \div +50^\circ$ with an accuracy of 0.5°. Specially made pick-up with curved legs was used (Fig.1) together with a constant-temperature hot-wire anemometer DISA-55D. Hot wire had 0.5mm- long working section with 5mkm diameter.

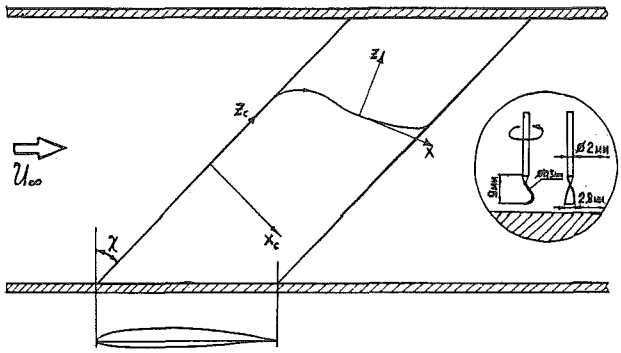

FIGURE 1. Scheme of the model mounted in the wind tunnel.

The measurements of different velocity vector components were based on the sensitivity of a hot-wire transducer to the angle between the local flow velocity vector and a hot-wire axis. The measurement procedure of three velocity vector components consisted in the recording of the signal values for three different angular positions of the hot-wire (-30°, 0°, $+30^\circ$ with respect to the direction normal to the streamwise test section axis) and in a subsequent solution of three equations with three unknown values of velocity vector components. The equations included the calibration relationship between the effective velocity causing voltage variations in the measuring anemometer bridge, free-stream flow velocity vector and the angle between the wire and velocity vector. The analysis of the errors has shown that this method makes it possible to estimate only two velocity vector components with reasonable precision, namely, streamwise and cross flow components. The values of total measurement errors were 1.5% and 0.9% respectively for streamwise and cross flow components of the local velocity vector.

During china-clay visualization dark model surface coated by a thin layer of kaolin was moistened with slow-evaporating ether. In airflow the speed of evaporation depends on mass transfer in boundary layer which in turn is proportional to local skin friction. When a visualization picture is developed after some exposure in constant flow regime, surface color varies from dark (in locations where ether is not vaporized and wet kaolin coating is transparent) to white (in locations where ether is vaporized and dry kaolin coating is white). Exposure time can be chosen so that not only transition line is clearly seen as in classical china-clay method /13/, but also variations of color in laminar boundary layer show the influence of cross flow instability.

Test results

Fig.2 shows measured pressure distributions on the model upper surface for different angles of attack and $V\infty$ = 40m/s in the section depicted in Fig.1.

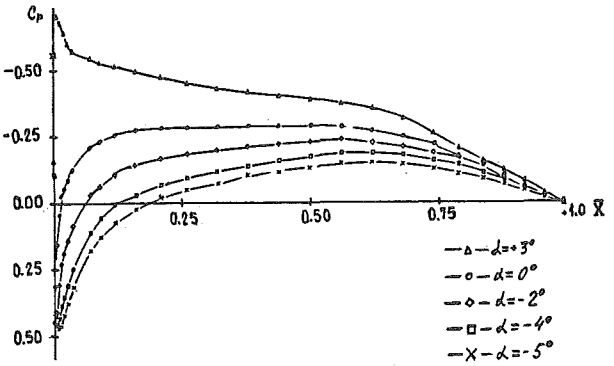

FIGURE 2. Measured pressure distributions on the wing upper surface. $V\infty$ = 40 m/s.

At zero incidence china-clay visualization results did not show any indications of stationary disturbances in the velocity range 20 ÷ 90 m/s (Re = $0.7 \div 3 \cdot 10^6$). The transition on the upper model surface occurred downstream of the laminar separation or as a result of Tollmien-Schlichting instability developement (Fig.3a).

At α = 3 the flow with forward suction peak occurred on the upper surface with maximum suction value increasing spanwise towards rear wing sections. The spanwise transition location was extremely non uniform due to this suction peak growth, the laminar separation being notified at rear sections (Fig.3b).

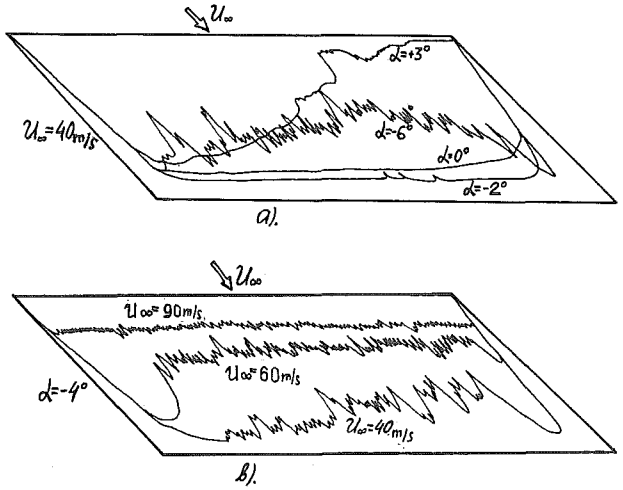

FIGURE 3. Drawings obtained from china-clay transition patterns: a) V_∞ = 40 m/s, α = var; b) $\alpha = -4^\circ$, $V\infty$ = var.

Well discernible stationary disturbances were detected on the upper model surface at negative angles of attack lower than $\alpha = -2^\circ$. At incidence $\alpha = -2^\circ$ and $V\infty$ = 40m/s, several bright narrow strips appeared on the china-clay coating approximately at x/b = 0.2 and spread to a slightly curved transition line without saw teeth. As velocity grew up to 60 m/s, the number of strips increased, but the transition line did not move forward essentially, the transition taking place, as before, downstream of the laminar separation. At V = 60 m/s strips occupied the full span of model upper

surface. For greater velocities the cross flow instability began to play important role in the transition process, the transition line took a characteristic saw-toothed shape and began to move forward as V increased (Fig.3a). This figure also shows that as wing incidence decreases causing stronger negative pressure gradient at constant Reynolds number, the transition line moves to the trailing edge if the laminar separation (or longitudinal instability) dominates and to the leading edge if the cross flow instability plays a key role.

The main volume of experimental information was obtained at $\alpha = -4^\circ$ and velocity range (V = 20 ÷ 90 m/s). In this case an extended region with a rather strong negative streamwise pressure gradient occurring on the upper surface caused essential cross flow instability development. A system of alternating bright and dark strips appeared on the china-clay coating in the laminar zone starting approximately at x/b = 0.1 (V = 90 m/s) to 0.2 (V = 40 m/s). Some of strips gave origin to turbulent wedges which expanded, joined and formed a characteristic saw-toothed transition line (Fig.3b) limiting the length of the rest of strips. As V raised the number of these turbulent wedges increased and the scatter in a wedge apex x-position decreased, i.e., the spanwise transition pattern became more periodical.

Fig.4 shows some measurement results of the mean period of stationary disturbances λ_c along Z_c-axis which was estimated by means of the calculations of the number of strips on the 200mm-long region. The distance between adjacent strips varied from 0.5 to 1.5 λ_c at the same X-coordinate, which corresponds to the conclusion of /6/ that there were unstable stationary disturbances within a rather wide range of wave numbers. Chordwise variation of the mean period resulted visually from disappearance of some strips and the confluence of two adjacent strips into one strip.

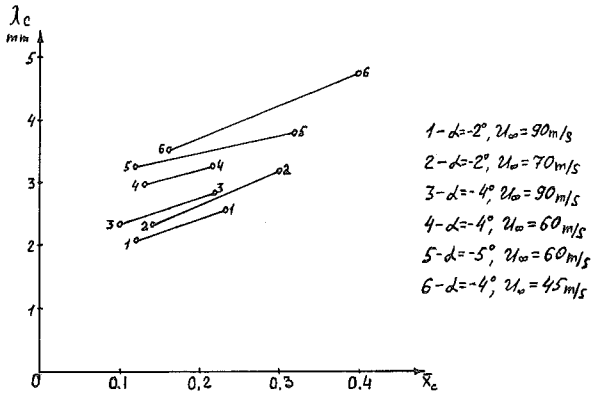

FIGURE 4. Span-averaged period of stationary disturbances.

Fig.5 shows mean transition locations at $\alpha = -5^\circ$ incidence and different velocities (V = 40 ÷ 90 m/s). Vertical bars near experimental points correspond to average lengths of saw-teeth in transition line. Measured freestream flow turbulence level is written for reference near each experimental point.

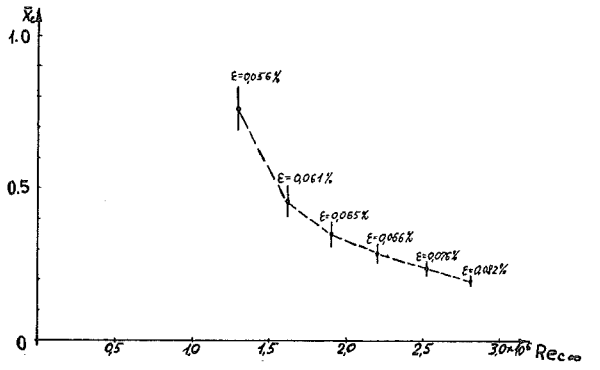

FIGURE 5. Span-averaged transition location.

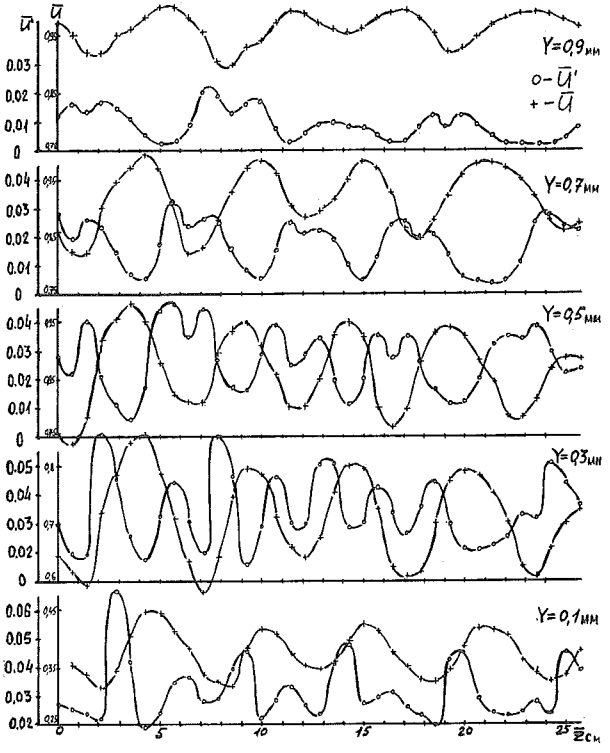

FIGURE 6. Time mean and RMS fluctuations of streamwise velocity at several distances from the wall. V∞ = 40 m/s, $\alpha = -4^\circ$, X/b = 0.4

Hot-wire anemometer measurements in the boundary layer were carried out at $\alpha = -4^\circ$, V = 40m/s, x/b = 0.4. First, a transducer with a wire oriented in parallel to the surface and perpendicularly to the test section longitudinal axis was moved along the Z-axis at several fixed distances from the model surface (Y = 0.1, 0.3, 0.5, 0.7, 0.9 mm). In this case, r.m.s. fluctuation values and time mean values of the effective velocity acting on the transducer were measured. The results of these measurements are presented in Fig.6, where the plots show spanwise distributions of velocity and its fluctuations which are normalized by the velocity at the boundary layer outer edge. Comparison of mean velocity and fluctuations distributions with china-clay visualization results shows that the mean velocity maxima

correspond to the most deep minima in the velocity fluctuations distributions and to the middles of bright strips on china-clay coating. Mean velocity minima correspond to local, less deep minima in the r.m.s. fluctuations distributions and to the middles of dark strips on china-clay coating. Maxima of r.m.s. fluctuations correspond to merging regions between dark and white strips. The spanwise period of oscillations for all distances from the surface coincided with the period of the strip structure on the china-clay coating.

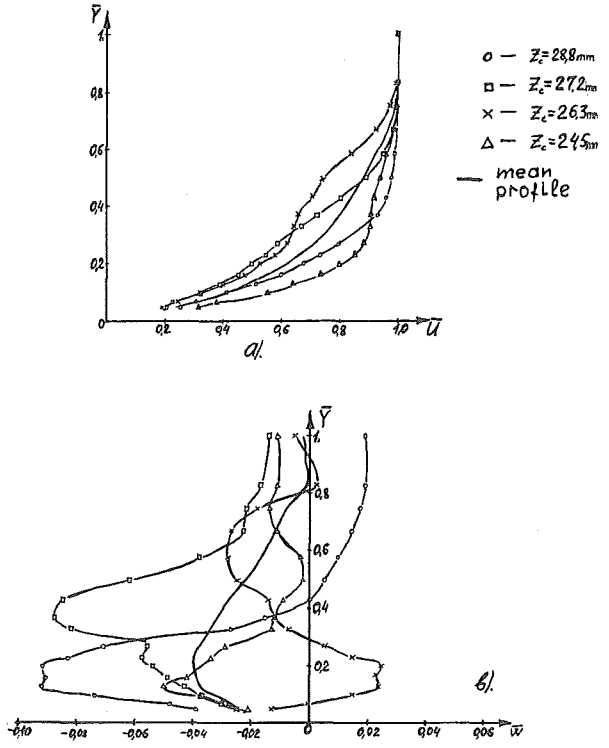

FIGURE 7. Streamwise (a) and crossflow (b) velocity profiles. ——— - spanwise averaged profiles.

To measure cross flow velocity profiles the hot wire was placed at given Xc, Zc at a minimum possible distance from the model surface and then it was moved upwards with a given step. Measurements at three angular positions were performed for each step giving after processing described above the streamwise and cross flow mean velocity profiles. Four given locations Xc, Zc were used so that the hot wire should pass through the axes of two adjacent vortices and between them (Fig.9). These profiles are shown in Fig.7a,b as well as span-averaged profiles of streamwise and cross flow velocity vector components. After the span-averaged profiles were subtracted from the local mean profiles, resulting profiles of stationary disturbances were plotted (Fig.8,9) whose form corresponded well to calculated (/5/-/8/) form of stationary disturbances: streamwise vortices with the rotation direction alternating spanwise (Fig.9). It should be noted that the cross flow velocity disturbances (7% of the velocity outside boundary layer) exceeded the maximum span-averaged cross flow velocity value (4%), while the amplitude of the streamwise velocity disturbances reached 20%.

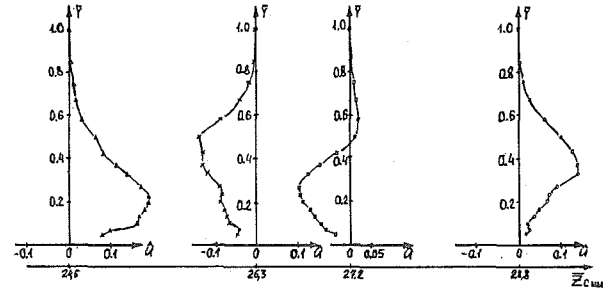

FIGURE 8. Streamwise velocity disturbance profiles.

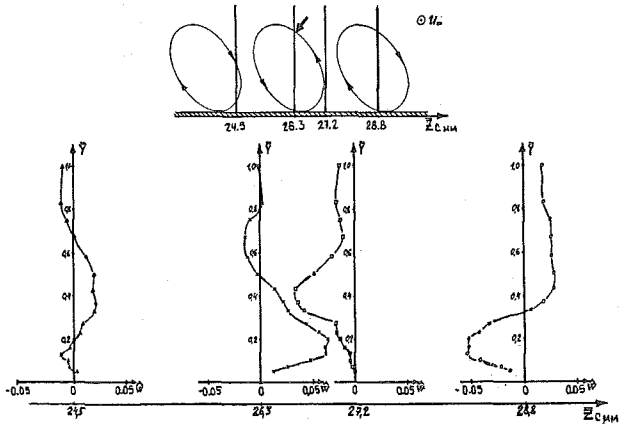

FIGURE 9. Crossflow velocity disturbance profiles.

After a more careful investigation of the visualization pattern it turned out that turbulent wedges forming the transition line originated at the boundaries between bright and dark strips, i.e. in the vicinity of the vortex axes, bright and dark strips being respectively to the right and to the left of the vortices developing to turbulent wedges if viewed streamwise. This indicated that the vortices transforming to turbulent wedges have the same rotation direction, namely they are the vortices with induced near-wall cross flow velocities directed backwards with respect to mean (span-averaged) boundary layer cross flow. Streamwise velocity profile across the boundary layer was extremely inflected near the center of this vortex (Fig.7a). This can lead to a secondary instability and to earlier local turbulization compared to adjacent vortices which was observed in the experiment.

Hot-wire signal spectra showed high amplitudes of low frequencies. Small oil drops on the wing surface had wavy trajectories clearly noticeable at a final stage of the stationary vortices development. The low-frequency oblique waves typical for cross flow instability seem to be a possible explanation of the effect.

Linear cross flow stability calculations /12/ showed rather wide interval of transition N-factor values due to freestream turbulence level. For minimum turbulence level N-factor in transition varied between 7.5 and 8.5.

References

[1] D.Arnal, J.C.Juillen: Three Dimensional Transition Studies at ONERA/CERT. AIAA-87-1335, 1987

[2] Gray W.E.: The effect of wing sweep on laminar flow. RAE TM 255 (1952).

[3] Owen P.R., Randall D.G.: Boundary Layer Transition on a swept back wing. RAE TM 256 (1953).

[4] Gregori W., Stewart J.T., Walker W.S.: On the stability of three-dimensional boundary layers with application to the flow due to a rotating disk. Phil. Trans. A248 (1955).

[5] D.Arnal, H.Habiballah, E.Coustols: Theorie de l'instabilite laminair et criteres le transition en ecouliment bi-et tridimensionnel. La Recherche Aerospatiale, N 2 1984.

[6] U.Dallman, U.Bieler: Analys and simplified prediction of primary instability of 3-D boundary layer flows. AIAAp-87-1337.

[7] Zhigulev V.N., Tumin A.M.: Turbulence Onset. "Nauka", Novosibirsk, 1987 (in Russian).

[8] Arnal D., Coustols E., Juillen J.C.: Etude experimental et theorique de la transition sur une aile en fleche infinie. La Recherche Aerospatiall, 1984, N 4.

[9] W.S.Saric, L.G.Yeats. Experiments on the stability of crossflow vorticies on swept wing flows. AIAAp-85-0493.

[10] U.Bippes, P.Nitschke-Kowsky: Experimental study of instability modes in a three-dimensional boundary layer. AIAAp-87-1336.

[11] D.Arnal, J.C.Juillen.: Experimental and theoretical studies of transition in incompressible three-dimensional flows. Boundary Layer Instability and Transition. University of Exeter, England, 1987, 21-25 Sept. Programme Details and Abstracts of Papers.

[12] Karas O.V., Kovalev V.E., Kuparev V.E.: Determination of laminar-turbulent transition point on a swept wing. Utcheniye zapiski TsAGI, v.XX, N.6, 1989 (in Russian).

[13] E.J.Richards, F.H.Burstall.: The China Clay Method of indicating transition position. ARC R&M 2126, 1945